Surface and corrosion properties of Type 430 ferritic stainless steel in parsley (*Petroselinum Sativum*) essential oil-containing sulphuric acid solution

To cite this article: Omotayo Sanni *et al* 2021 *Surf. Topogr.: Metrol. Prop.* **9** 045050

Surface Topography: Metrology and Properties

PAPER

Surface and corrosion properties of Type 430 ferritic stainless steel in parsley (*Petroselinum Sativum*) essential oil-containing sulphuric acid solution

RECEIVED
2 November 2021

REVISED
7 December 2021

ACCEPTED FOR PUBLICATION
14 December 2021

PUBLISHED
24 December 2021

Omotayo Sanni , Jianwei Ren and Tien-Chien Jen

Department of Mechanical Engineering Science, University of Johannesburg, Cnr Kingsway and University Roads, Auckland Park, 2092, Johannesburg, South Africa

E-mail: tayo.sanni@yahoo.com

Keywords: ferritic stainless steel, adsorption, corrosion, parsley essential oils, corrosion inhibitor

Abstract

This study examined the corrosion inhibiting properties of parsley (*petroselinum sativum*) essential oils, for Type 430 ferritic stainless steel in 0.5 molar sulphuric acid solutions. In this study, weight loss, electrochemical and scanning electron microscope techniques were used in gaining a detailed understanding of inhibition effects of parsley (*petroselinum sativum*) essential oils (PEO) on Type 430 ferritic stainless steel corrosion. The inhibitor studied exhibits good anti-corrosion performance with 98.65% inhibition efficiency. This result could be ascribed to the adsorbed PEO on the surface of the stainless steel, and this was verified by surface visualization using optical and scanning electron microscope techniques while the crystallographic variation of the inhibited sample is studied by x-ray diffraction (XRD). The adsorption of PEO onto stainless steel surface is controlled by Langmuir adsorption isotherms. Optical images of non-inhibited specimens showed a severely corroded surface with a visible macro pit on the stainless steel from sulphuric solutions. The inhibited sample shows improved surface owing to the surface protection effect of PEO molecules. The corrosion inhibition performance of PEO is due to the presence of active constituents which enhanced the film formation over the surface of the metal, thus, mitigating corrosion.

1. Introduction

Sulphuric acid is frequently utilized for industrial acid pickling, refining crude oil, oil-well acid in petrochemical processes and oil recovery, and acid cleaning of stainless steel. The destructive nature of sulphuric acid accelerates the steel deterioration in contact with them. The issue results from the wide industrial applications of steel in building and construction, chemical processing, oil refinery, mining, automobile, energy generation, petrochemical, and marine industries. During application, the steel shows weak corrosion resistance owing to its incapability to passivation in aggressive media. The formed oxide on the steel is porous which allows the corrosion process to continue on the steel. Thus, enormous damage does occur resulting in corrosion, high costs of repair, and maintenance.

Corrosion problem is constant and continuous, often difficult to eliminate. Its prevention would be more achievable and practical than complete elimination. In most situations, corrosion of metal can be slowed, managed, or stopped with an appropriate technique. Appropriate corrosion control can significantly reduce or prevent the effect of corrosion on steel such as the use of inhibitors. Different organic and inorganic compounds as corrosion inhibitors for metal in different aggressive environments have been reported in the literature [1–16]. However, the exorbitant prices of the organic compounds and the toxic nature of most inorganic inhibitors are the main setback for their continuous usage. Due to the clarion call for green chemistry, the search for effective inhibitors for metal corrosion in different aggressive environments has recently taken a new dimension. Also, because the whole idea of protecting metals against corrosion is attached to environmental sustainability, and economic benefit, therefore, substances used as corrosion inhibitors must be environmentally friendly, readily available, and cheap.

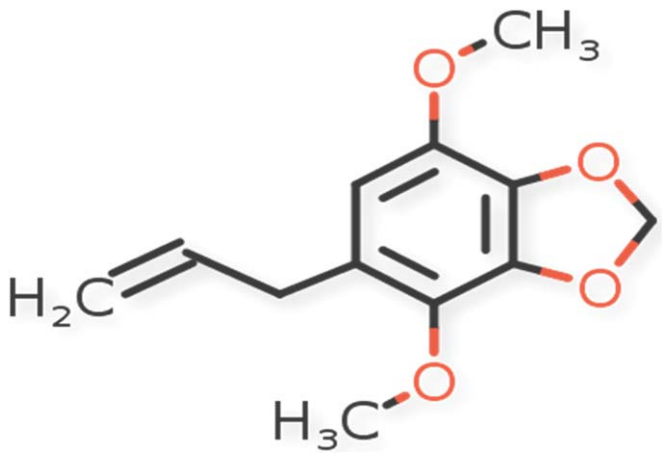

Figure 1. Chemical structure of the PEO.

Thus, research activities are geared towards replacing toxic and expensive inorganic and organic corrosion inhibitors. Eco-friendly, non-toxic, natural at 'zero' or low environmental impact are preferred. Essential oils [17–20] have shown excellent inhibitive efficiency for corrosion of steel in corrosive solutions. Nevertheless, little research has been carried out on the Type 430 ferritic stainless steel corrosion inhibition in sulphuric acid media by PEO. The environmental threat by most synthetic inhibitors is the main reason to study the possibility of essential oils as corrosion inhibitors. Natural oils are obtained from renewable resources, environmentally friendly, readily available, and are inexpensive. Nevertheless, PEO has not been studied as an inhibitor for Type 430 ferritic stainless steel in sulphuric acid solutions to the best of our knowledge. Stainless steel Type 430 is one of the most popular steel used in corrosion resistant and high strength applications. Acid solutions are generally used for the removal of undesirable rust and scale in several industrial processes, the highly corrosive nature of aqueous acids on stainless steel Type 430 requires some degree of restraint to achieve maximum safety conditions, economic maintenance and minimum loss of materials. Given this, the aim of this study was to examine the corrosion inhibiting properties of parsley (*petroselinum sativum*) essential oils, for Type 430 ferritic stainless steel in 0.5 molar sulphuric acid solutions by electrochemical and weight loss techniques. Also, the characterization of the samples was performed by optical microscopy (OPM), scanning electron microscopy (SEM), and x-ray diffraction (XRD) analysis.

2. Experimental

2.1. Materials

The parsley essential oil used in this study was of pure quality (>99%) and used without purification. The chemical structure of this compound is indicated in figure 1. The composition (wt%) of the Type 430 ferritic stainless steel utilized in this study is Si 0.182, C 0.05, S 0.017, Ni 1.3, Cu 0.102, P 0.12, Mn 1.83, Cr 13, and Balance Fe. The ferritic stainless steel was mechanically press-cut into samples of 2 cm × 2 cm dimensions for weight loss measurements. The 0.5 molar sulphuric acid was prepared by diluting an analytical grade of H_2SO_4 (98%) with distilled water and used as the corrosive test environment.

2.2. Weight loss analysis

Ferritic stainless steel Type 430 with 10 cm^2 surface area, in triplicate, was immersed in aerated 250 ml of 0.5 M H_2SO_4 solutions with and without different PEO concentrations. The samples were dipped in a 250 ml beaker containing sulphuric acid medium with and without PEO concentrations with the aid of a glass hook and rod, after accurately weighing via digital balance with ±0.1 mg sensitivity. The temperature was controlled by a water thermostat. The corrosive acid solution was open to the air throughout the experiment. The weight of the sample before and after immersion to the corrosive medium was recorded using an analytical balance. After each immersion time, the samples were removed, wash with a bristle brush under running water to eliminate the corrosion products, dried, and reweighed correctly following ASTM G31–72 [21]. The plot of corrosion rates and inhibition efficiency was plotted from the obtained data during the immersion time. The corrosion rate in mm/year and inhibition efficiency was calculated according to equations (1) and (2) [22]:

$$CR = \left[\frac{87W}{DAT}\right] \quad (1)$$

W (mg) indicates weight loss, A (cm^2) FSS surface area, D (g cm^{-3}) FSS density and T (hour) immersion time. Equation (2) was used in calculating the inhibition efficiency (IE):

$$IE = \left[\frac{CR - CR_0}{CR}\right] \times 100 \quad (2)$$

CR_0 and CR are the FSS corrosion rates in inhibited and uninhibited acid solutions.

2.3. Electrochemical study

For the polarization measurements, standard corrosion glass cells were used. The working electrode is a ferritic stainless steel sample with a 1 cm^2 surface area. The reference and counter electrodes are silver-silver chloride (Ag/AgCl) and platinum sheet, respectively. The samples were finely polished with diamond paste to get a mirror-like surface. After polishing, the steel coupons were washed and rinsed with ethanol and distilled water, respectively, and dried in the air, and finally stored in a desiccator before test according to ASTM G1–03 [23]. It was then transferred to the glass cells with 250 ml of the corrosive solution. To reduce ohmic contributions, the reference electrode was kept close to the ferritic stainless steel surface embedded in a PVC holder with epoxy resin so that the exposed surface was the only working electrode surface. The electrochemical polarization was recorded 30 min after the working electrode was immersed in the test solutions, to stabilize the stationary potentials. The potentiodynamic current potential curve was recorded by changing automatically the electrode potential from −1.5 V to 1.5 V at a scan rate of $1mVs^{-1}$ according to ASTM G102–89 [24]. The TAFEL linear segment of the anodic and cathodic curves was extrapolated to corrosion potential to obtain the corrosion current densities.

2.4. Surface analysis

Stainless steel samples immersed in the solution with optimum concentration of inhibitor and without inhibitor in the test solution for 168 h were removed and rinse with running water. After rinsing, the sample was dried and analyzed with optical and scanning electron spectroscope techniques. The structure of the inhibited and uninhibited samples was characterized using x-ray diffraction analysis performed by x-ray diffractometer with Cu Kα radiation.

3. Results and discussion

3.1. Weight loss measurement

3.1.1. Effect of concentration

The weight-loss technique in monitoring the rate of corrosion is useful owing to its reliability and simple applications. Plots of ferritic stainless steel (FSS) corrosion rate and inhibition efficiency versus exposure time at specific PEO concentration are shown in figures 2 and 3. Shown in figure 5 is the optical image at different magnifications of FSS after 168 h of immersion in H_2SO_4 without PEO, and after 168 h immersion in H_2SO_4 solution with PEO (600 ppm). The corrosion rate versus exposure time plot (figure 2) without PEO differs significantly from the plots with PEO concentrations owing to the electrochemical action of SO_4^{2-} anions according to equation (3) [25]:

$$Fe(s) + H_2SO_4(aq) \rightarrow FeSO_4(aq) + H_2O(g) \quad (3)$$

The mechanism of corrosion reaction results in accelerated corrosion and severe oxidation of the FSS surface as presented in the optical images (figure 5) where the degree of deterioration of the FSS surface from H_2SO_4 solutions is high compared to the sample with PEO. A noticeable decrease in the FSS rate of corrosion value with immersion time is owing to the weakening of the static acid electrolyte with discharged corrosion product. Thus, the corrosion rate of FSS without PEO culminated at 12.32477 mm $y^{-1}e^{-1}ar^{-1}$ and 8.182356 mm $y^{-1}e^{-1}ar^{-1}$ in H_2SO_4 solution. PEO at 200 ppm concentration in H_2SO_4 solution was notably inadequate to slow down the FSS corrosion as presented in the corrosion rate values after 144 h. Figure 2 shows a significant increase in the rate of corrosion at a lower concentration. At 400 ppm PEO concentration, a notable decrease in the rate of corrosion occurred resulting in 1.09999 mm $year^{-1}$ at 168 h. At 1000 ppm concentration of PEO, corrosion rate value of 0.2400 mm $year^{-1}$ was achieved at 168 h suggesting effective corrosion inhibition. The inhibitive performance of FSS with different PEO concentrations in 0.5 molar sulphuric acid solutions at different time of exposure is presented in figure 3. From figure 3, inhibition efficiency values increase clearly with increasing PEO concentrations, that is, the inhibitor concentration enhances the corrosion inhibition. This behavior is due to the increase in inhibitor coverage and adsorption on the metal surface with the inhibitor concentration [26]. Observation of PEO inhibition efficiency with immersion time plots in the acid solution indicates the effective performance of PEO in H_2SO_4 solutions. At 24 h of exposure, the inhibitive performance of PEO in H_2SO_4 solutions at 200 ppm concentration was 87%. However, considerable inhibition values in H_2SO_4 occurred from 400 ppm PO concentration (97%). At 1000 ppm PEO concentration, an optimum value of 98.65% was achieved after 24 h. General observation explains that PEO at high concentrations in H_2SO_4 solution decreases with exposure time, though the reduction rate is minimal till around 120 h to 168 h where the relative stability and progressive increase was noticed. The high inhibition efficiency of PEO implies a high bonding ability of inhibitor on the surface of the ferritic stainless steel.

3.1.2. Effect of immersion time

Weight loss test was carried out in the acid solution without and with PEO at different concentrations, to evaluate the steadiness of inhibitor film adsorbed at the acid solution/ferritic stainless steel interface with exposure time. The maximum inhibition efficiency of 98.65% and 98.05% was observed from figure 3 for 168 h of immersion period in 0.5 M H_2SO_4. The

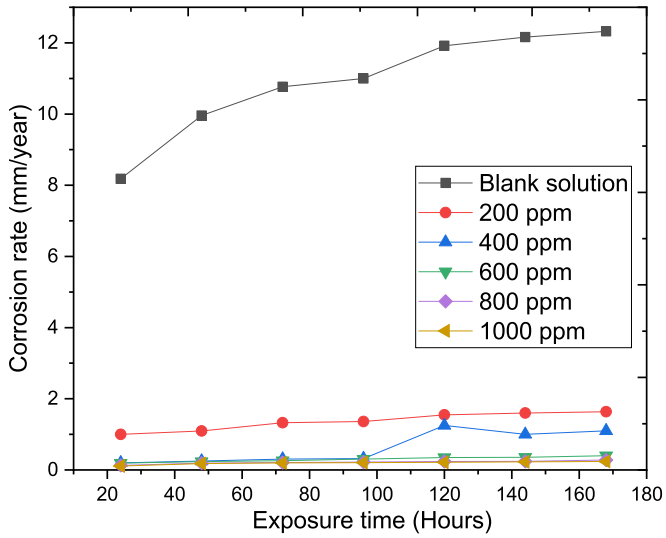

Figure 2. Plot of corrosion rate versus exposure time in 0.5 M H_2SO_4 solutions.

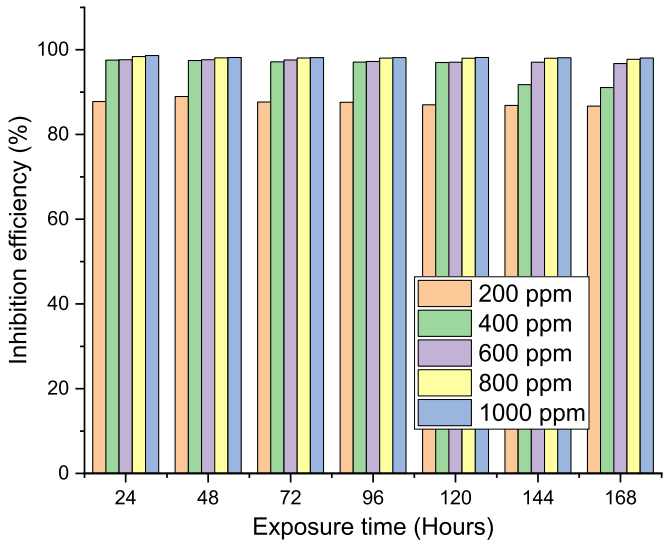

Figure 3. Plot of inhibition efficiency as a function of exposure time in 0.5M H_2SO_4 solution.

immersion study reveals that as the immersion time increased the inhibitor efficiency slightly decreases. After 96 h, a slight decrease in the efficiency of the inhibitor yielding 87.61% and 98.13 at 200 and 1000 ppm respectively was observed, and then later stabilized. This observation can be explained owing to the increase of inhibitor molecules adsorbed on the surface of the FSS with exposure time. The decrease in inhibitive performance with exposure time could be owing to the essential oil desorption from the surface of the FSS [27]. Messikh *et al* [28] explained that a decrease in inhibitor efficiency over a long period of time may be ascribed to the inhibitor molecules depletion in the solutions owing to the chelate formed between the inhibitor ligands and the metal. The inhibitor efficiency stability at 168 hours signifies that PEO is a promising corrosion inhibitor for FSS in 0.5 molar sulphuric acid solutions at different time of immersion.

3.1.3. Effect of temperature

The temperature effect on the inhibition performance of the inhibitor studied was carried out, weight loss measurement was investigated in the temperature range 298 K−318 K, and the result is shown in figure 4. With an increase in a temperature range from 298 K to 318 K, it is expected that the inhibitor efficiency decreased with temperature; however, in the present study, the corrosion rates of the studied inhibitor was found to reduce with temperature, signifying that the inhibitor process of adsorption on the FSS surface is exothermic. The inhibition efficiency was found to

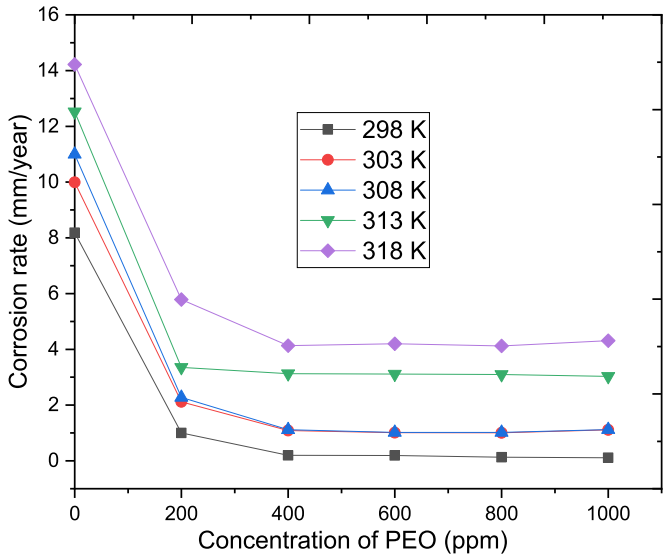

Figure 4. Variation of corrosion rate with concentration at various temperatures.

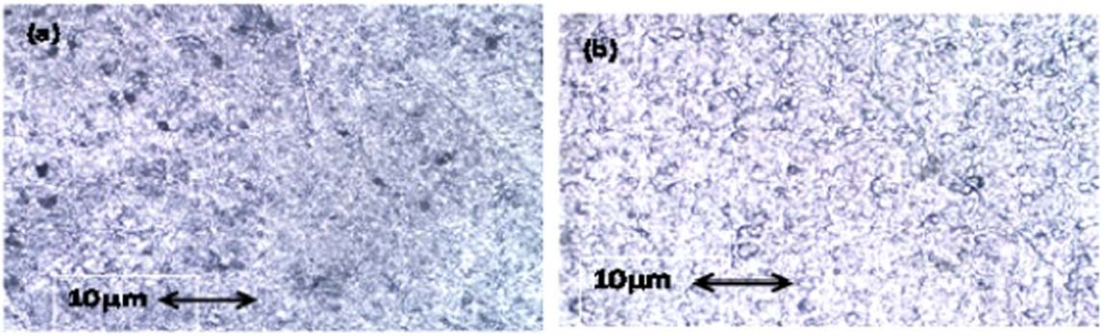

Figure 5. Optical images of FSS after corrosion test in 0.5 M H_2SO_4 solution (a) without and (b) with inhibitor.

decrease in 0.5 molar sulphuric acids. Further temperature rise, decreased the inhibitor efficiency but at higher concentrations the decrease was minimal.

Figure 3 further shows that, the inhibitor efficiency increased with increasing PEO concentrations but slightly decreased as the temperature increases. The decrease in the PEO efficiency with temperature may be ascribed to the adsorbed oil components on the surface of the ferritic stainless steel. Therefore, it is pertinent to conclude that the high inhibitive performance of the essential oil in this study could be ascribed to the high phytochemical constituent in the essential oil. In addition, the presence of O, C as shown in the chemical structure of PEO serves as the adsorption site of the essential oil onto the FSS surface, therefore enhances the FSS protection from the corrosive agent in the aqueous solutions. This observation could be clarified as: desorption and adsorptions of the inhibitor molecule occur continuously at the steel surface and at an exact temperature, equilibrium exists between the two processes. The equilibrium between desorption and adsorption process is shifted with the increase in temperature resulting in high desorption than adsorption rate till equilibrium is attained again at diverse equilibrium constant values. This clarifies the low inhibitor performance at high temperatures [29]. The obtained corrosion rates values with temperature show that the PEO adsorbed on the surface of the steel is physical at higher and low temperatures; chemical adsorption may also take place.

3.2. Electrochemical measurement

The effect of the studied inhibitor on the polarization and corrosion behavior of the FSS was investigated in 0.5 M H_2SO_4 solution. Anodic-cathodic polarization of the FSS in the presence and absence of PEO in 0.5 M H_2SO_4 has been performed and presented in figure 6. The entire analysis of the polarization curve was done and the electrochemical corrosion data of corrosion rate, corrosion current densities (i_{corr}), corrosion potential (E_{corr}), cathodic Tafel slope (β_c), and anodic Tafel slope (β_a) as a function of PEO concentrations, are shown in table 1. Accordingly, the corrosion current densities value is accurately estimated by

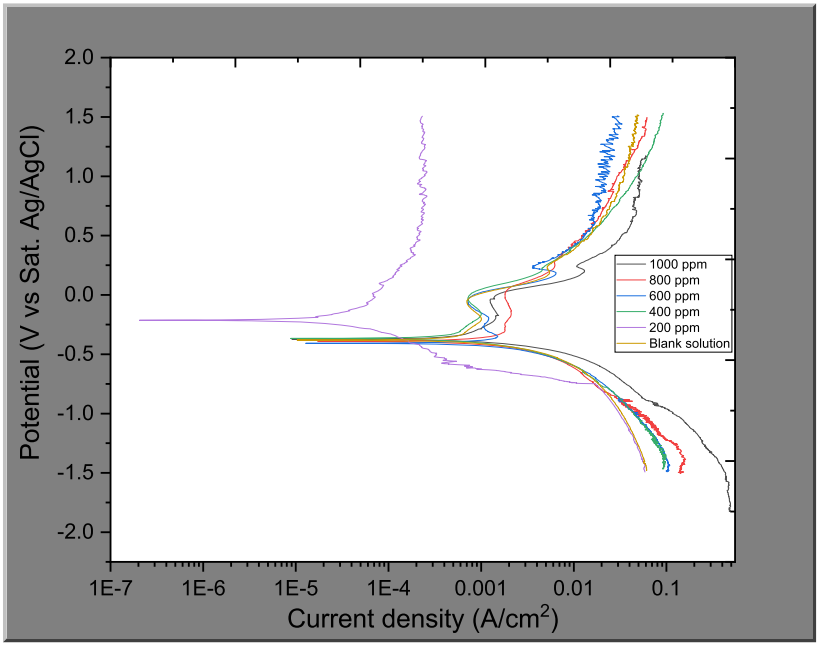

Figure 6. Potentiodynamic polarization curves for FSS in 0.5 M H_2SO_4 with and without different concentrations of PEO.

Table 1. Potentiodynamic polarization parameters for the corrosion of FSS in 0.5 M H_2SO_4 solutions with different concentrations of PEO.

Concentration (ppm)	β_c(V dec^{-1})	β_a(V dec^{-1})	I_{corr} (A cm^{-2})	Polarization resistance (Ω)	E_{corr}(V)	Corrosion rate (mm year^{-1})	Inhibition efficiency (%)
Blank solution	0.21177	0.42562	0.000531	32.267	−0.38809	6.1703	—
200	0.14375	0.15872	0.000391	40.997	−0.38776	4.5389	84
400	0.10611	0.10795	0.000358	83.866	−0.38515	4.1595	93
600	0.037744	0.090035	0.000247	94.023	−0.36299	2.8721	95
800	0.18516	0.068736	0.000143	974.88	−0.35533	1.6621	97
1000	0.022757	0.032814	5.99E-06	1617.3	−0.15672	0.0696	98

extrapolating the cathodic linear region back to the corrosion potentials. The Tafel line region indicates that the presence of PEO compounds often shifted the anodic and cathodic lines to lower current density with the PEO concentrations indicating that this compound is a mixed-type inhibitor. With the presence of 1000 ppm, the corrosion current density value decreased from 0.000531 A cm^{-2} to 5.99E-06 A cm^{-2} for the PEO, respectively. Also, the corrosion rate values decrease with inhibitor concentrations, because of the increase in the blocked fraction of the surface of the electrode by adsorption. No noticeable drastic change in the Tafel cathodic values indicating that the mechanism of hydrogen evolution did not change with the presence and absence of the inhibitor. At a high concentration of the inhibitor, the anodic values decreased, indicating a change in the metal dissolution mechanism. The presence of the inhibitor at the studied concentrations decreases gradually the current densities with an increase in the PEO concentrations. The corrosion rate value decreases drastically with the presence of PEO, indicating that PEO is an excellent inhibitor for FSS in 0.5 M sulphuric acid media. The parsley essential oil is capable of selective adsorption like other inhibitors, that is, they are adsorbed on the inner portion of the electrical double layers. The substances adsorbed shift most of the positively charged ions from the outer Helmholz plane, thereby limiting the ease of access of the surface of the metal for the reactive positive ion. Indicating, the essential oil blocks the surface of the metal and so the reaction rate of the hydrogen evolution reduces, and thus the overall corrosion reaction rate decreases. It was inferred that the parsley essential oil is a mixed-type inhibitor and its inhibitive performance is due to simple geometric blocking mechanisms [30]. Obtained values from weight loss test and potentiodynamic polarization curves are in good agreement.

3.3. Adsorption consideration

The main step in the action of most organic corrosion inhibitors in the acid environments has been considered to be adsorption at the solution-metal interface. The degree of surface coverage parameter plays a major role in the evaluation of inhibitor behavior and is used to fit data from the experiment to adsorption isotherms to have a better understanding of the inhibition mechanism. PEO fits Langmuir adsorption

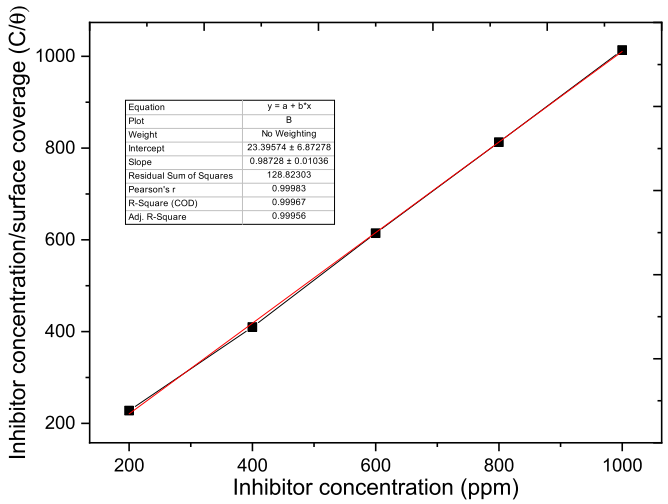

Figure 7. Langmuir adsorption isotherm with PEO in the acid solution.

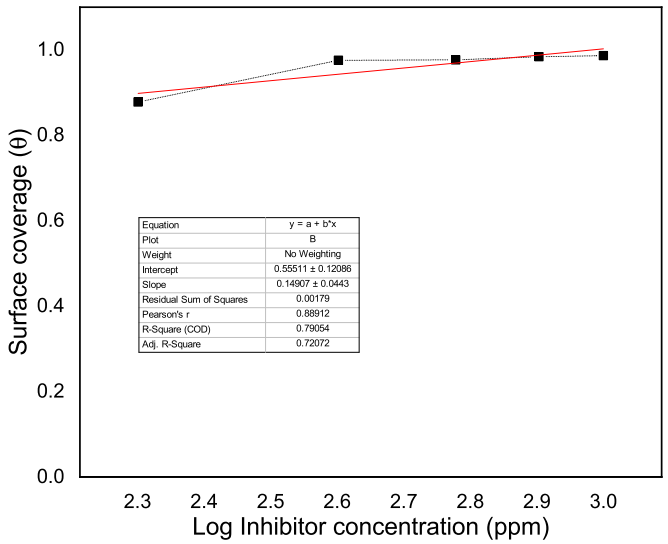

Figure 8. Temkin adsorption isotherm with PEO in the acid solution.

isotherms with straight lines for the log C versus log (θ/1-θ) plots. The obtained straight line shows that adsorption is the main process of inhibition. This observation explains that the increase in inhibitor performance with concentrations indicate that the oil substituent's component number adsorbed increased over the FSS surface blocks the active site, where direct acid attack proceed and protect the steel from corroding, whereas diminished inhibitor performance with temperature suggests physical adsorption (electrostatic interaction of the essential oil phytochemical constituent) on the surface of the FSS forming a protective film and thus shields the steel from corroding.

3.3.1. Langmuir isotherm

To deduce whether there is formation of an insoluble complex layer on the metal surface acting as a barrier between the corrosive medium and the surface of the metal usually termed as physisorption, the Langmuir adsorption isotherms were used. The Langmuir plots describe the relationship between the inhibitor concentration and the metal surface coverage. The Langmuir adsorption isotherms can be express as [31],

$$\frac{C}{\theta} = \frac{1}{K} + C \tag{4}$$

Where C is the inhibitor concentration, θ is the degree of surface coverage, and K adsorption equilibrium constant. The logarithms of equation (4) yield:

$$Log(C/\theta) = \log C - \log K \tag{5}$$

The plot of C/θ versus C are linear as presented in figure 7 with R^2 value of 0.999. The R^2 value and slope is approximately unity, denoting strong adherence to the Langmuir adsorption isotherms. The suitability of the studied inhibitor to the Langmuir adsorption isotherm denotes no interaction between the adsorbent and the adsorbate [32, 33].

Table 2. Thermodynamic data's of FSS with the presence of PEO in the acid solution.

Concentration (ppm)	Ea kJ mol^{-1}	Free energy of adsorption $-\Delta G$ (kJ mol)$^{-1}$ at different temperature range					$-\Delta S$ kJ mol^{-1}	ΔH kJ mol^{-1}
		298 K	303 K	308 K	313 K	318 K		
Blank solution	62						32	13
200	60	14.85	15.99	15.88	17.70	18.96	31	13
400	57	14.79	15.96	15.77	17.61	18.74	30	13
600	55	14.51	15.95	15.51	17.24	18.74	30	13
800	52	14.49	15.92	15.48	17.31	18.22	30	12
1000	51	14.46	15.91	15.42	17.27	18.17	30	12

3.3.2. Temkin isotherms

The concentration of the inhibitor (C) is linked with the degree of surface coverage (θ) in the Temkin adsorption isotherm following equation (6) [34]:

$$Exp(-2a\theta) = KC \tag{6}$$

Where K is the adsorption equilibrium constant and a is the attractive parameter. Equation (7) [34] is obtained by rearranging and taking the logarithm of equation (6).

$$\theta = -2.303 \log K/2a - 2.303 \log C/2a \tag{7}$$

The plot of surface coverage versus the logarithm of concentration as presented in figure 8 gives an R^2 value of 0.79054 denoting that PEO strongly obeys Langmuir adsorption better.

3.4. Activation energies

The apparent activation for the corrosion process is estimated from Arrhenius plots following equation (8) [35]:

$$W = K_{\exp} Ea/RT \tag{8}$$

Where Ea is the apparent activation corrosion energy, T absolute temperature, k is the Arrhenius pre-exponential constant, and R universal gas constant. Table 2 shows the Arrhenius values for the FSS corrosion. The apparent activation energy (Ea) values of hydrogen evolution reactions for uninhibited FSS in sulphuric acid solutions agree with the data reported in the literature on the activation energy for steel in acidic solutions [31]. The existence of PEO modified the Ea values; this modification can be ascribed to the mechanism change of the process of corrosion with the PEO adsorbed molecules [36]. The decrease in inhibitive performance of PEO with an increase in temperature and a corresponding increase in activation energy values in the inhibited solutions compared to uninhibited solutions is interpreted often as being indicative of the physical adsorbed layer formed [37]. The authors [38] attributed the lower activation energies value to inhibitor adsorption slow rate with a resultant closer approach to equilibrium during the experiment at high temperatures. While the decrease in corrosion activation energies at a high level of inhibition occurs from shifting the net corrosion reactions from the parts not covered on the surface of the metal to the covered ones was explained by [39]. The authors [40] found that organic molecule inhibits the cathodic and anodic partial reaction on the surface of the electrode and parallel reactions take place on the areas covered, while, the reaction rates on the areas covered is considerably less than the areas uncovered.

3.5. Thermodynamic parameters

Thermodynamic parameters: ΔG, ΔS, and ΔH, were calculated from the temperature study results. Table 2 shows the obtained values at different temperatures for the PEO concentrations. The obtained negative free energy of adsorption values denotes the adsorption spontaneity process and the stable adsorbed layer on the metal surface. The negative values of ΔG more than -40 (KJmol^{-1}) involves transfer or charge sharing from the molecules of the inhibitor to the surface of the metal to form a co-ordinate bond type indicating the chemical type of adsorption while the ΔG values up to -20 (KJmol^{-1}) are generally consistent with electrostatic interactions between a charged metal and the charged molecules, and the adsorption process denotes physical adsorption [41]. The ΔG values vary from -15.2 to -19.4 in 0.5 M H_2SO_4 in the present study indicating that PEO functions by adsorbing physically onto the metal surface**.** The result of electrostatic attraction between the charged species in the bulk solution and the charged surface of the metal is physisorption. The negatively charged adsorption species is eased if the metal surface is positively charged, and the positively charged species can as well protect the positively charged surface of the metal which acts with a negatively charged intermediate, such as acid anion adsorbed on the surface of the metal. Though, physisorption is the main contributor whereas chemical adsorption contributed slightly to the adsorption mechanism as a result of the decrease in the inhibitor performance with an increase in temperature [42]. In this study, the temperature effects and ΔG values on the FSS corrosion with the presence of PEO in the sulphuric acid solution support the physical process of adsorption on the surface of FSS. The ΔS and ΔH values were calculated from equation (9).

$$\Delta G = \Delta H - T\Delta S \tag{9}$$

The entropy of adsorption (ΔS) and enthalpy of adsorption (ΔH) values are calculated from the plots of ΔG versus T. The positive values of the enthalpy

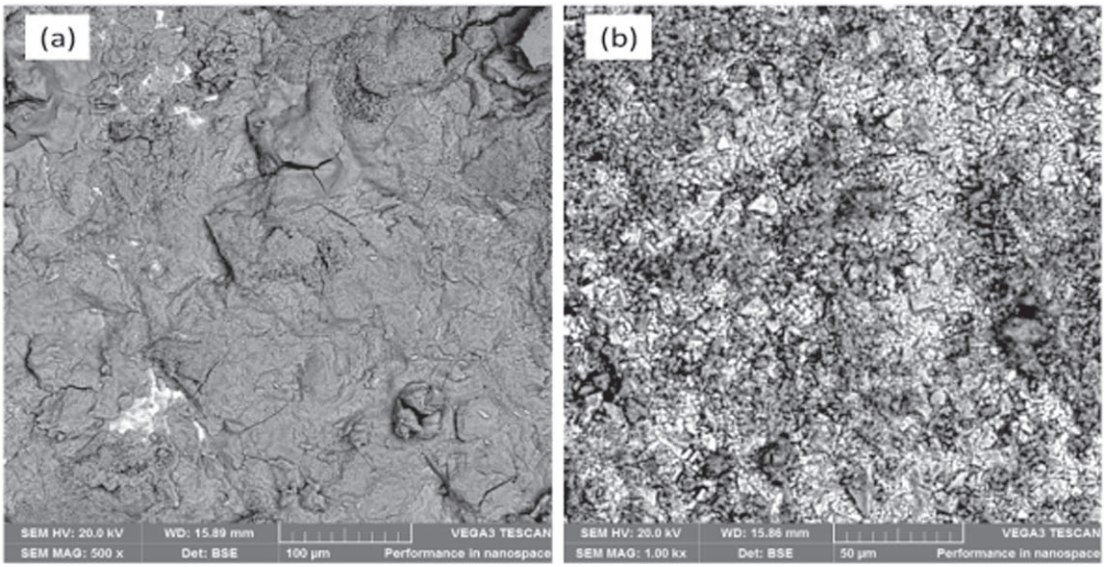

Figure 9. SEM micrograph of ferritic stainless steel immersed in acid solution (a) without PEO (b) with PEO.

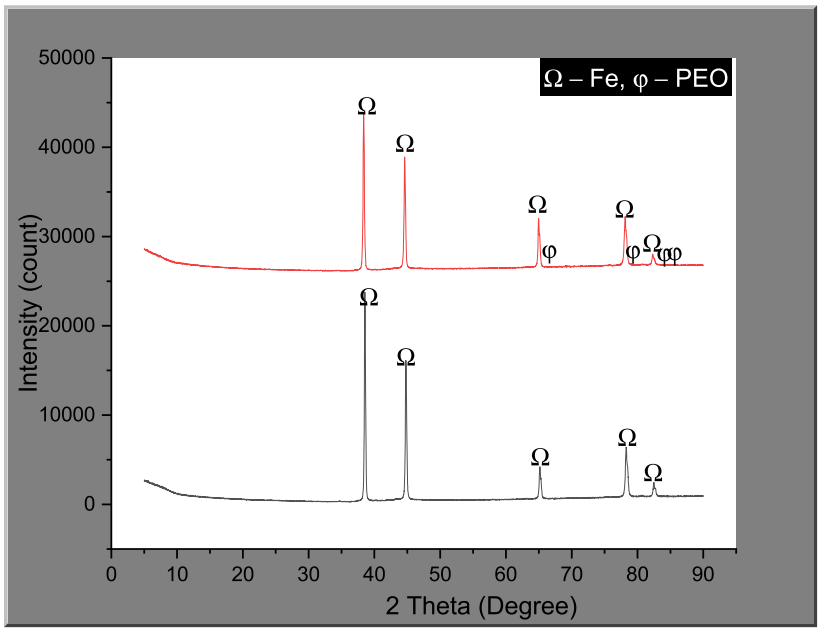

Figure 10. XRD spectra of ferritic stainless steel samples with and without inhibitor.

with the PEO reflect the endothermic nature of the FSS process of dissolution signifying that the metal dissolution is difficult [37, 43]. The entropies (ΔS) negative values with the presence of PEO in the acid solutions shows that the PEO molecule, moving freely in the bulk solutions was orderly adsorbed on the surface of FSS. This observation shows that the activation complex in the rate-determining steps signifies the association step than the dissolution steps, signifying that a decrease in disordering occurs from the reactant to the activated complex [44]. The changes in ΔS and ΔH with inhibitor concentration imply that the process is entropic and enthalpic controlled.

3.6. Surface analysis

The scanning electron microscope (SEM) image was recorded to ascertain the interactions of the inhibitor molecule with the surface of FSS. The SEM image of the FSS specimens after 168 h of immersion in 0.5 M H_2SO_4 solutions in the absence and presence of 1000 ppm (optimum concentration) of PEO is shown in figure 9. The SEM images show clearly that the corrosion reaction does not occur homogeneously over the FSS surface in 0.5 molar sulphuric acid solutions. In the uninhibited solutions, the specimen undergoes general corrosion as shown in figure 9(a),

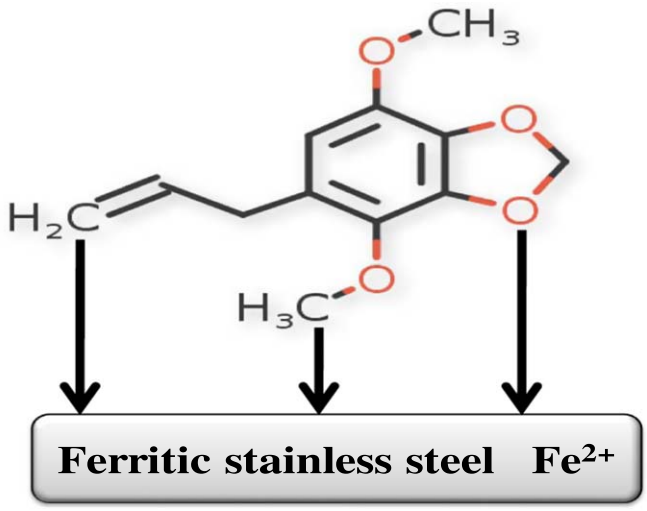

Figure 11. Proposed scheme for adsorption of PEO on the Type 430 ferritic stainless steel in 0.5M H_2SO_4 solutions.

where the entire surface was highly attacked. The PEO present in the solution prevents the corrosion in the inhibited solutions; a slight attack shows on the metal surface (figure 9(b)). In the case of the inhibited solutions, the specimen is free of attack but the polish scratch on the specimen still appears. However, the surface is remarkably protected by the essential oil in comparison to the inhibitor-free solution. Figure 10 shows the XRD patterns of inhibited and uninhibited ferritic stainless steel samples. The XRD spectra show the presence of austenitic phases and found no traces of diffraction peaks of secondary phases; nitrides or carbides precipitations. The XRD patterns of the samples show the same diffraction peaks but the peak intensity ratios are different for inhibited and uninhibited samples, due to the PEO film form on the inhibited sample. The XRD results also show that both samples have the ferritic structure, which is a body-centered cubic structure [45]. The inhibited sample depicts a more dominant austenite phase due to its high inhibition protection of PEO on the steel surface. The high dominant austenite phase in the inhibited sample is due to the reduced grain growth owing to the existence of a stable PEO layer on the steel surface. An additional peak at $2\theta = 82^\circ$ formed could be due to reactions of different elements present in the stainless steel composition with oxygen or each other due to SO_4^{2-} in the corrosive solution that may act as a catalyst.

3.7. Inhibition process

The essential oils are composed of different naturally occurring organic compounds with C and O atoms in their functional group and O-heterocyclic ring, and these act as reaction centers resulting in film formation on the steel surface. This compound may be protonated in the test solutions; therefore, the inhibitive behavior of PEO might be attributed to the PEO components adsorbed on the steel surface [46]. The corrosion inhibition performance of natural compounds is mainly because of the presence of complex organic species. This organic compound contains a polar function with O and C, and conjugated double bond or aromatic ring in their molecular structure, which is the main adsorption center [41]. In addition, the anti-corrosion performance is ascribed to the heterocyclic constituents present in the PEO which form adsorbed films on the metal surface. The first stage of the inhibition process in this study is electrostatic adsorption which occurred between the negatively charged metal surface and the cationic species. The adsorbed organic molecule orientation at the surface of the metal is significant, suggesting the molecules are adsorbed physically via the positively charged atom and the aromatic ring parallel to the surface of the metal. Therefore, the PEO molecules will cover a large area of the surface of the metal. This is evident by the high inhibition performance of the essential oil, especially at low concentrations. The PEO compound physisorption is also evident from the larger negative value of ΔGads and the lower value of Ea, with the presence of the inhibitor compound and the decrease in inhibition efficiency values with temperature. We assume that the formed complex between the metal surface and the essential oil molecules occurs owing to the inhibitor molecules' adsorption on the FSS surface. The adsorption layer serves as a barrier between the aggressive solution and the metal surface. The results from the different techniques used suggest the same order for inhibition efficiency, denoting the consistency in the experimental data. Assigning a general mechanism of action to an inhibitor is often impossible since the action of the mechanism could change with experimental conditions. Therefore, the major inhibitor mechanism in acid solution may vary with different factors: the inhibitor concentration, the nature of the acid anion, the nature of the metal, and other species present in the solution [42]. In the

present study the mode of adsorption considered can be summarized as:

i. The protonated PEO may adsorb through electrostatic interactions between the negatively charged surface of the metal and the positively charged molecules. A coordinate bond may be formed by partial transfer of an electron from the polar atom (O atom) to the metal surface when protonated PEO is adsorbed on the surface of the steel. Also, due to the lone-pair electron of O atoms in PEO or protonated PEO may combine with Fe^{2+} ion freshly generated on the surface of the steel to form a metal-inhibitor complex [31].

$$Fe \rightarrow Fe^{2+} + 2e^{-} \quad (10)$$

$$PEO + Fe^{2+} \leftrightarrow [PEO - Fe]^{2+} \quad (11)$$

$$[PEO_x]^{x+} + Fe^{2+} \leftrightarrow [PEO_x - Fe]^{(2+x)+} \quad (12)$$

Sruthi *et al* [16] proposed a similar type of mechanism. This complex may be adsorbed onto the surface of the steel by Vander Waal forces forming a protecting layer to retard FSS against corrosion. The efficient inhibition of the PEO could also be owing to the phytochemical constituent large size of the essential oil covering a wide area of the surface of the metal thereby minimizing the rate of corrosion.

ii. The neutral PEO could be adsorbed onto the FSS surface via the physisorption mechanisms, involving the displacement of water molecules from the FSS surface and the sharing electrons between the O atoms and Fe (see figure 11).

4. Conclusions

Based on the obtained results from the electrochemical and weight loss measurement, the following conclusions are drawn: Parsley essential oil effectively inhibited the corrosion of Type 430 ferritic stainless steel in 0.5 M H_2SO_4 solutions. The inhibition efficiency increases with inhibitor concentration, and the maximum efficiency of 98.65% was achieved at 1000 ppm concentration of the essential oil. The corrosion rate of the steel increases with temperature, signifying the adsorption of the oil on the metal surface is physisorption and fits the Langmuir adsorption isotherm. The negative free energy of adsorption denotes spontaneous and strong PEO adsorption on the surface of the steel. The potentiodynamic polarization test shows that PEO affects the cathodic and anodic Tafel slope which suggests that the inhibitor acted as a mixed-type inhibitor.

Acknowledgments

The financial support from University of Johannesburg, Johannesburg, South Africa is highly acknowledged.

Data availability statement

All data that support the findings of this study are included within the article (and any supplementary files).

ORCID iDs

Omotayo Sanni https://orcid.org/0000-0001-6979-795X

References

[1] Verma C, Ebenso E E and Quraishi M 2020 Molecular structural aspects of organic corrosion inhibitors: influence of–CN and–NO_2 substituents on designing of potential corrosion: inhibitors for aqueous media,' *J. Mol. Liq.* **316** 113874

[2] Verma D K, Dewangan Y, Dewangan A K and Asatker A 2021 Heteroatom-based compounds as sustainable corrosion inhibitors: an overview *Journal of Bio-and Tribo-Corrosion* **7** 1–18

[3] Boughoues Y, Benamira M, Messaadia L and Ribouh N 2020 Adsorption and corrosion inhibition performance of some environmental friendly organic inhibitors for mild steel in HCl solution via experimental and theoretical study *Colloids Surf., A* **593** 124610

[4] Quraishi M, Chauhan D S and Ansari A F 2021 Development of environmentally benign corrosion inhibitors for organic acid environments for oil-gas industry, *J. Mol. Liq.* **329** 115514

[5] Erami R S, Amirnasr M, Meghdadi S, Talebian M, Farrokhpour H and Raeissi K 2019 Carboxamide derivatives as new corrosion inhibitors for mild steel protection in hydrochloric acid solution, *Corros. Sci.* **151** 190–7

[6] Boughoues Y, Benamira M, Messaadia L, Bouider N and Abdelaziz S 2020 Experimental and theoretical investigations of four amine derivatives as effective corrosion inhibitors for mild steel in HCl medium, *RSC Adv.* **10** 24145–58

[7] Sayin K and Karakaş D 2013 Quantum chemical studies on the some inorganic corrosion inhibitors, *Corros. Sci.* **77** 37–45

[8] Deyab M, Eddahaoui K, Essehli R, Rhadfi T, Benmokhtar S and Mele G 2016 Experimental evaluation of new inorganic phosphites as corrosion inhibitors for carbon steel in saline water from oil source wells *Desalination* **383** 38–45

[9] Samiee R, Ramezanzadeh B, Mahdavian M and Alibakhshi E 2019 Assessment of the smart self-healing corrosion protection properties of a water-base hybrid organo-silane film combined with non-toxic organic/inorganic environmentally friendly corrosion inhibitors on mild steel *J. Clean. Prod.* **220** 340–56

[10] Shinato K W, Zewde A A and Jin Y 2020 Corrosion protection of copper and copper alloys in different corrosive medium using environmentally friendly corrosion inhibitors *Corros. Rev.* **38** 101–9

[11] Bashir S, Thakur A, Lgaz H, Chung I-M and Kumar A 2020 Corrosion inhibition efficiency of bronopol on aluminium in 0.5 M HCl solution: Insights from experimental and quantum chemical studies *Surfaces and Interfaces* **20** 100542

[12] Bashir S, Thakur A, Lgaz H, Chung I-M and Kumar A 2020 Corrosion inhibition performance of acarbose on mild steel corrosion in acidic medium: an experimental and computational study *Arab. J. Sci. Eng.* **45** 4773–83

[13] Bashir S, Thakur A, Lgaz H, Chung I-M and Kumar A 2019 Computational and experimental studies on Phenylephrine as anti-corrosion substance of mild steel in acidic medium *J. Mol. Liq.* **293** 111539

[14] Fadhil A A, Khadom A A, Ahmed S K, Liu H, Fu C and Mahood H B 2020 Portulaca grandiflora as new green corrosion inhibitor for mild steel protection in hydrochloric

acid: quantitative, electrochemical, surface and spectroscopic investigations *Surfaces and Interfaces* **20** 100595
[15] Yuce A O 2020 Corrosion inhibition behavior of Robinia pseudoacacia leaves extract as a eco-friendly inhibitor on mild steel in acidic media *Met. Mater. Int.* **26** 456–66
[16] Sruthi G, Shakeela K, Shanmugam R and Rao G R 2020 The corrosion inhibition of stainless steel by ferrocene–polyoxometalate hybrid molecular materials–experimental and first principles studies *Phys. Chem. Chem. Phys.* **22** 3329–44
[17] Abdallah M, Zaafarany I, Khairou K and Emad Y 2012 Natural oils as corrosion inhibitors for stainless steel in sodium hydroxide solutions *Chem. Technol. Fuels Oils* **48** 234–45
[18] Hossain S, Razzak S and Hossain M 2020 Application of essential oils as green corrosion inhibitors, *Arab. J. Sci. Eng.* **45** 1–23
[19] Bouraoui M M, Chettouh S, Chouchane T and Khellaf N 2019 Inhibition efficiency of cinnamon oil as a green corrosion inhibitor *Journal of Bio-and Tribo-Corrosion* **5** 28
[20] Cisse K, Gassama D, Thiam A, Bathily M and Fall M 2021 Evaluation of the inhibitory effectiveness of cyperus articulatus essential oils on the corrosion of structural steelwork in hydrochloric acid solution *Chemistry Africa* **4** 379–90
[21] ASTM STANDARDS 2004 Standard practice for laboratory immersion corrosion testing of metals **03.02** G31–72
[22] Sanni O and Popoola A P I 2019 Data on environmental sustainable corrosion inhibitor for stainless steel in aggressive environment *Data in brief* **22** 451–7
[23] ASTM G1–03 Standard Practice for Preparing 2003 *Cleaning, and evaluating corrosion test specimens astm international, west conshohocken. USA*
[24] ASTM STANDARDS 2004 Standard practice for calculation of corrosion rates and related information **03.02** G102–89
[25] Adejo S O, Yiase S G, Leke L, Onuche M, Atondo M V and Uzah T T 2019 Corrosion studies of mild steel in sulphuric acid medium by acidimetric method *International Journal of Corrosion and Scale Inhibition* **1** 50–61
[26] Hameed R S A, Al-Bagawi A, Shehata H A, Shamroukh A H and Abdallah M 2020 Corrosion inhibition and adsorption properties of some heterocyclic derivatives on C-steel surface in HCl *Journal of Bio-and Tribo-Corrosion* **6** 1–11
[27] Satpati S, Suhasaria A, Ghosal S, Saha A, Dey S and Sukul D 2021 Amino acid and cinnamaldehyde conjugated Schiff bases as proficient corrosion inhibitors for mild steel in 1 M HCl at higher temperature and prolonged exposure: detailed electrochemical, adsorption and theoretical study *J. Mol. Liq.* **324** 115077
[28] Messikh S, Salhi R, Benali O, Ouici H and Gherraf N 2020 Synthesis and evaluation of 5-(Phenyl)-4H-1, 2, 4-triazole-3-thiol as Corrosion Inhibitor for Mild Steel in 0.5 MH2so4 and its synergistic effect with potassium iodide *Inter. J. Chem. Biochem. Sci* **17** 14–38
[29] Farha0dian A, Rahimi A, Safaei N, Shaabani A, Abdouss M and Alavi A 2020 A theoretical and experimental study of castor oil-based inhibitor for corrosion inhibition of mild steel in acidic medium at elevated temperatures *Corros. Sci.* **175** 108871
[30] Hsissou R, Benhiba F, Dagdag O, El Bouchti M, Nouneh K, Assouag M, Briche S, Zarrouk A and Elharfi A 2020 Development and potential performance of prepolymer in corrosion inhibition for carbon steel in 1.0 M HCl: outlooks from experimental and computational investigations *J. Colloid Interface Sci.* **574** 43–60
[31] Leelavathi S and Rajalakshmi R 2013 Dodonaea viscosa (L.) leaves extract as acid corrosion inhibitor for mild steel–a green approach *Journal of Materials and Environmental Science* **4** 625–38
[32] Shimizu S and Matubayasi N 2021 Adsorbate-adsorbate interactions on microporous materials *Microporous Mesoporous Mater.* **323** 111254
[33] Al-Ghouti M A and Da'ana D A 2020 Guidelines for the use and interpretation of adsorption isotherm models: A review *J. Hazard. Mater.* **393** 122383
[34] Eddy N O and Ebenso E E 2008 Adsorption and inhibitive properties of ethanol extracts of Musa sapientum peels as a green corrosion inhibitor for mild steel in H_2SO_4 *African Journal of Pure and Applied Chemistry* **6** 046–54
[35] Zhou L, Peng T, Sun H and Hui T 2021 Mechanism and kinetics of iron removal in Fe-Al-H_2SO_4 system by coordination precipitation *J. Environ. Chem. Eng.* **4** 105241
[36] Yadav D K, Quraishi M and Maiti B 2012 Inhibition effect of some benzylidenes on mild steel in 1 M HCl: an experimental and theoretical correlation *Corros. Sci.* **55** 254–66
[37] Chung I-M, Malathy R, Kim S-H, Kalaiselvi K, Prabakaran M and Gopiraman M 2020 Ecofriendly green inhibitor from Hemerocallis fulva against aluminum corrosion in sulphuric acid medium *J. Adhes. Sci. Technol.* **34** 1483–506
[38] Benali O, Larabi L, Merah S and Harek Y 2011 Influence of the methylene blue dye (MBD) on the corrosion inhibition of mild steel in 0.5 M sulphuric acid, Part I: weight loss and electrochemical studies *J. Mater. Environ. Sci* **2** 39–48
[39] Tsoeunyane M, Makhatha M and Arotiba O 2019 Corrosion inhibition of mild steel by poly (butylene succinate)-L-histidine extended with 1, 6-diisocynatohexane polymer composite in 1 M HCl *International Journal of Corrosion* **2019**
[40] Fouda A, El-Dossoki F, El-Hossiany A and Sello E 2020 Adsorption and anticorrosion behavior of expired meloxicam on mild steel in hydrochloric acid solution *Surf. Eng. Appl. Electrochem.* **56** 491–500
[41] Kutluay S, Baytar O and Şahin O 2019 Adsorption kinetics, equilibrium and thermodynamics of gas-phase toluene onto char produced from almond shells *Res Eng Struct Mater* **5** 279–98
[42] Zinad D, Jawad Q, Hussain M, Mahal A, Mohamed L and Al-Amiery A 2020 Adsorption, temperature and corrosion inhibition studies of a coumarin derivatives corrosion inhibitor for mild steel in acidic medium: gravimetric and theoretical investigations *Int. J. Corros. Scale Inhib* **9** 134–51
[43] Husaini M, Usman B and Ibrahim M B 2020 Study of corrosion inhibition performance of Glutaraldehyde on Aluminium in nitric acid solution *Algerian Journal of Engineering and Technology* **2** 003–010
[44] Chioma F, Nnenna O W and Moses O 2020 Preparation, spectral characterization and corrosion inhibition studies of (E)-N-{(Thiophene-2-yl) methylene} pyrazine-2-carboxamide schiff base ligand *Protection of Metals and Physical Chemistry of Surfaces* **56** 651–62
[45] Kapoor M, Isheim D, Ghosh G, Vaynman S, Fine M E and Chung Y-W 2014 Aging characteristics and mechanical properties of 1600 MPa body-centered cubic Cu and B2-NiAl precipitation-strengthened ferritic steel *Acta Mater.* **73** 56–74
[46] Foda A, Mosallam H, El-Khateeb A and Fakih M 2019 Cinnamomum zeylanicum Extract as Green Corrosion Inhibitor for Carbon Steel in Hydrochloric Acid Solutions *Progress in Chemical and Biochemical Research* **2** 120–33